Supporting information

Bone-Targeted ICG/Cyt c@ZZF-8 Nanoparticles Based on the Zeolitic Imidazolate Framework-8: A New Synergistic Photodynamic and Protein Therapy for Bone Metastasis

Zichao Jiang[1,3,4]*, Yixiao Pan[1,3,4]*, Jiahao Wang[1,3,4], Jingyi Li[1,3,4], Haoze Yang[6], Qi Guo[1,3,4], Shuailong Liang[1,3,4], Sijie Chen[7], Yihe Hu[2,4]†, Long Wang[1,3,4,5]†

[1]Department of Orthopedics, Xiangya Hospital, Central South University, China, [2]Department of Orthopedics, First Affiliated Hospital, School of Medicine, Zhejiang, China, [3]University Hunan Engineering Research Center of Biomedical Metal and Ceramic Implants, Xiangya Hospital, Central South University, China, [4]National Clinical Research Center for Geriatric Disorders, Xiangya Hospital, Central South University, Changsha, China, [5]Hunan key laboratary of aging biology, Xiangya Hospital, Central South University, Changsha, China, [6]Department of Cardiology, Second Xiangya Hospital, Central South University, China, [7]Department of Ultrasound Diagnosis, Second Xiangya Hospital, Central South University, China.

*: These authors contributed equally to this work, †: Corresponding to Long Wang, MD, Ph.D., E-mail: dr_wanglong@csu.edu.cn and Yihe Hu, MD, Ph.D. E-mail: huyh1964@163.com

Experiment section

1. Characteristics and Detection of ICG/Cyt c@ZZF-8 NPs

The size distribution and zeta potential of the ICG/Cyt c@ZZF-8 NPs and other NPs (dispersed in DI water) were analyzed by a Malvern size and zeta potential analyzer (Malvern Nano ZS, UK) at room temperature (20°C). Then, NP size was measured at certain time points after dispersion in 10% fetal bovine serum (FBS) to observe their stability. The morphology of the ZIF-8 NPs and ICG/Cyt c@ZZF-8 NPs was characterized by transmission electron microscopy (TEM) (Hitachi H-7600), and TEM elemental mappings were also performed to observe the distribution of Zn, S, C, N, O and P elements in the ICG/Cyt c@ZZF-8 NPs. The absorption spectra of the free ICG solution, Cyt c solution, ZZF-8 and ICG/Cyt c@ZZF-8 NPs (0.2 ml of each sample, equivalent ICG concentration of 3.30 μg/ml, ZZF-8 concentration at 50 μg/ml) were measured by a steady-state spectrophotometer (BioTek Instruments, UK). The Fourier transform infrared (FT-IR) spectra of Cyt c, ZIF-8 and ICG/Cyt c@ZZF-8 NPs were obtained using an FT-IR spectrophotometer (Spectrum Two, Perkin Elmer). The drug-loading and encapsulation efficiency were determined by a direct method, and the total weight of the ICG/Cyt c@ZZF-8 NPs was measured after freeze-drying and complete dissolution in ethylenediaminetetraacetic acid (EDTA). The released ICG was quantitated by absorbance at 780 nm, Cyt c was quantitated by the catalytic conversion rate of 3-ethylbenzthiazoline-6-sulfonic acid (ABTS) in H_2O_2 solution at an absorbance intensity of 417 nm (we measured at an absorbance intensity of 417 nm instead of 734 nm to avoid interference from the ICG absorption peaks). The test solution for Cyt c was prepared by mixing 100 μL of collected sample solution (decomposed NP solution) with 400 μL of H_2O_2 (0.8 mM) and 500 μL of ABTS (1 mg/mL) for 1 h at room temperature. Drug-loading and encapsulation efficiencies were calculated according to the following formulae:

Drug loading (%) = $W_{drug}/W_{NPs} \times 100\%$

Encapsulation efficiency (%) = $W_{drug}/W_{added} \times 100\%$

2. Bone Targeting Ability of ICG/Cyt c@ZZF-8 NPs *in vitro*

Bone targeting ability *in vitro* was investigated by a hydroxyapatite (HPA) binding assay.[1] ICG/Cyt c@ZZF-8 NPs and ICG/Cyt c@ZIF-8 NPs were dispersed in DI water at a concentration of 1 mg/mL, and the initial absorbance was measured by a UV spectrophotometer at 780 nm. Then, 10 mg of HPA was added to 2 ml of ICG/Cyt c@ZZF-8 NPs and ICG/Cyt c@ZIF-8 NPs. Specifically, 10 mg of ZOL was incubated with 12 mg of HAP in 200 µl DI water (with the pH adjusted to 7) for 1 h, and the resulting ZOL-HAP was incubated with 2 mL of ICG/Cyt c@ZZF-8 NPs. The suspension was stirred for 5, 10, 20, 30, 60 and 120 min with an 8 min, 2000 rpm centrifugation step at each time point. A control group without HAP was used to evaluate the normal loss of NPs during the centrifugation process. All of the supernatants were collected and analyzed by a UV spectrophotometer at 780 nm, and the relative HPA binding percentage was determined according to the following equation:

$$\text{Relative HPA binding } (\%) = \frac{\text{Ab}_{\text{initial}} - \text{Ab}_{\text{supernatant}} - \text{Ab}_{\text{loss}}}{\text{Ab}_{\text{initial}}}$$

(Ab represents the absorbance at 780 nm)

3. The pH-related Release of ICG and Cyt c from ICG/Cyt c@ZZF-8 NPs *in vitro*

The pH-related properties of ICG/Cyt c@ZZF-8 NPs were tested using a standard method as follows: 100 µl ICG/Cyt c@ZZF-8 NPs (1 mg/ml) were suspended in 500 µl phosphate-buffered saline (PBS) at pH 7.4 and 5.0. The samples were placed in a 37°C shaker at 200 rpm and 500 µl supernatant was collected after centrifugation (10000 rpm, 7 min) at appropriate time points (0.5, 1, 2, 4, 6, 8, 12, 24 and 48 h). Released ICG and Cty c levels were quantitated by measuring absorbance at 780 nm and ABTS catalytic conversion rates, respectively.

4. ROS Generation Evaluation *in vitro*

Singlet oxygen sensor green (SOSG) was used to probe for ROS in solution. SOSG binds highly selectively with $^1O_2$ and does not visibly react with other reactive oxygen species (ROS), such as hydroxyl radicals and nitric oxide[2, 3]. One microliter of SOSG (5 mmol) in methanol was mixed with a solution of free ICG, ZIF-8 NPs, ICG@ZZF-8 NPs and ICG/Cyt c@ZZF-8 NPs (2 mL, 1 mg/mL, ICG concentration at 66 µg/ml). The solution mixture was irradiated with a 780 nm laser (0.5 W/cm^2) for different lengths of time (0, 1, 2, 3, 4 min). Then, the fluorescence intensities were recorded using a fluorescence spectrophotometer. ROS generation in the ICG and ICG/Cyt c@ZZF-8 NP solution was also tested under the same conditions in room light, and the relative $^1O_2$ production efficiency was determined by the following equation:

$$\text{Relative } ^1O_2 \text{ production efficiency} = F/F_0$$

F: fluorescence intensity peak value after laser irradiation,

F_0: fluorescence intensity peak value before laser irradiation.

To evaluate the generation of O_2 by H_2O_2 decomposition in the presence of ICG/Cyt c@ZZF-8 NPs, 1 mg/mL ICG/Cyt c@ZZF-8 NPs or ICG@ZZF-8 NPs were incubated with or without H_2O_2 solution (500 µM) and dissolved oxygen was subsequently measured using a portable oxygen meter

(AMT08, USA). Moreover, typically, the production of $^1O_2$ of ICG/Cyt c@ZZF-8 NPs after laser irradiation (0.5 W/cm^2, 4 min) with or without H_2O_2 (500 μM) under normal and hypoxic conditions were also tested by SOSG assays. Hypoxic conditions were simulated by saturation in a N_2 atmosphere for 30 min.

5. Cellular Experiment:

5.1 Cellular Uptake Investigation

To observe the cellular uptake of NPs, 1×10^4 4T1 cells were cultured on a glass-bottom dish (35 mm with intermediate aperture of 15 mm) for 24 h. Then, two groups of cells were added to 100 μl of a solution of ICG/Cyt c-FITC@ZZF-8 NPs and ICG/Cyt c-FITC@ZIF-8 NPs (1 mg/ml) and further incubated for 1 h, 2 h and 4 h. Afterward, the dish was washed with DI water three times, the cell nuclei were stained with DAPI, and the cells were imaged by confocal laser scanning microscopy. The excitation wavelengths of FITC and DAPI were 488 nm and 350 nm, respectively.

5.2 Intracellular ROS Generation Evaluation

DCFH-DA was used as the ROS fluorescence probe for imaging the intracellular ROS generation after ICG/Cyt c@ZZF-8 NPs treatment. A total of 1×10^4 4T1 cells in 200 μl culture medium were dropped into the center of 6-well plates, and the bottom of the well was filled with culture medium 3 h later. The cells were then incubated overnight and subsequently rinsed with cold PBS. The two groups of cells were treated with culture medium containing Cyt c, ICG, ICG@ZZF-8 NPs and ICG/Cyt c@ZZF-8 NPs for 4 h. One group of cells was exposed to an 800 nm laser (0.5 W/cm^2, 3 min), and the other group was kept in the dark in an incubator. Both groups of cells were imaged by confocal laser scanning microscopy with an excitation wavelength of 488 nm.

5.3 *In Vitro* Biocompatibility and Synergistic Therapy Evaluation

The biocompatibility of ZZF-8 NPs and the synergistic therapeutic effect of ICG/Cyt c@ZZF-8 NPs on tumor cells *in vitro* were evaluated by standard CCK-8 assays. First, different types of cells (4T1 cells, RAW264.7 mouse cells and HF-91 human cells) were incubated in a 96-well plate with 0.5×10^4 cells per well (0.1 ml medium) for 24 h (37℃, 5% CO_2). Then, ZZF-8 NPs at 0, 10, 20, 40, 60 and 80 μg/ml were added and the cells and NPSs were coincubated for another 24 h. Next, 10 μL of CCK-8 solution mixed with 90 μL of culture medium was added into the plate, which was further incubated for 30 min at 37℃. The absorbance intensity at 450 nm was measured with a microplate reader to measure cytotoxicity. The relative cell viabilities (%) were calculated and expressed as the means ± SD of five samples as follows: cell viability (%) = $OD_{sample}/OD_{control} \times 100\%$. The sample group was treated with NP solution, while the control group was treated with culture medium.

To verify that protein and photodynamic therapy can play a synergistic role in the treatment of tumor cells, 4T1 cells were treated with increasing concentrations of ICG, Cyt c, ICG@ZZF-8 NPs and ICG/Cyt c@ZZF-8 NPs (the total dose of ICG ranged from 0 to 3.30 μg/mL) for 4 to 5 h and with or without exposure to a 780 nm NIR laser (0.5 W/cm^2, 3 min). The cells were then further incubated for 24 h. The relative cell viabilities (%) were measured by CCK-8 assay as described above. To further confirm the synergistic anticancer effect, we determined the half-maximal inhibitory concentration (IC50) of ICG and Cyt c in the single therapy and combined therapy, for

determine the IC50 of ICG/Cyt c@ZZF-8 without laser group, we supplemented the experiments of this group, increased concentration of NPs at 60, 70, 80 and 90 μg/mL. Importantly, a combination index (CI) was used to evaluate the combined therapy in previous research[4, 5], and the CI was calculated according to the following formula:

$$CI = \frac{IC50_{(\text{ICG in combined therapy})}}{IC50_{(\text{ICG in single PDT})}} + \frac{IC50_{(\text{Cyt c in combined therapy})}}{IC50_{(\text{Cyt c in single protein therapy})}}$$

The effect of combined therapy is either synergism (CI < 1), additivity (CI = 1), or antagonism (CI > 1).

A live/dead cell staining assay using calcein-AM to stain live cells and propidium iodide (PI) to stain dead cells was used to directly observe the anticancer effect. 4T1 cells (1×10^5) were cultured on a glass-bottom dish (35 mm with an intermediate aperture of 15 mm) for 24 h, washed with PBS and incubated with free ICG, free Cyt c, ICG@ZZF-8 NPs and ICG/Cyt c@ZZF-8 NPs (at dose of ICG at 5.28 μg/mL) for 4 h. The cells were then exposed to a 780 nm laser (0.5 W/cm^2, 3 min) or remained untreated as the control. After incubation for another 12 h, the cells were incubated with calcein AM (5 μM) and PI solution (50 μM) for 20 min. Finally, the cells were observed by confocal laser scanning microscopy (CLSM, Zeiss LSM 510) with 488 nm excitation.

5.4 Invasion and Migration of Tumor Cells After Therapy *in vitro*

Transwell invasion and migration assays were used to evaluate the inhibition of migration and invasion capabilities of the nanoparticles. For the Transwell invasion assay, 100 μL Matrigel matrix (diluted to 50 μg/ml with serum-free DMEM medium) was added to a 24-well Transwell chamber (pore size: 8 μm) and incubated at $37^{\circ}C$ for 2 h to coat the chamber. 4T1 cells were then inoculated ($5x10^6$/ well) into the Matrigel-coated Transwell chambers after the following different treatments: 1) ICG/Cyt c@ZZF-8 with laser, 2) ICG@ZZF-8 with laser, 3) ICG/Cyt c@ZZF-8 without laser 4) ZZF-8 with laser, 5) free Cyt c solution with laser and the control group (concentration of NPs were equivalent at 40 μg/ml) with or without 780 nm laser exposure. One hundred microliters of RPMI-1640 medium containing 20% FBS was added to the lower chamber as attractant. The 4T1 cells were cultured for 24 h, and the Matrigel and the cells were subsequently removed from the upper chamber. The invading cells that adhered to the Transwell polycarbonate membrane were fixed with 4% paraformaldehyde for 60 min, stained with 1% crystal violet (Sigma) for 30 min, and washed three times with PBS. We evaluated the inhibition of NP invasion by calculating the number of cells on the polycarbonate membrane (random selection of 6 visual fields) using an inverted fluorescence microscope. For the Transwell migration assay, the Matrigel precoating step was omitted; all other steps were the same as those used in the invasion experiment. The invasive or migrating cells in the polycarbonate membrane were further quantified by ImageJ software.

6.*In Vivo* Experiments:

6.1 Establishment of Animal Model of Bone Metastasis

All animal experiments were approved and performed in strict accordance with the guidelines of the Animal Ethics Committee of Xiangya Hospital of Central South University in China. The mouse model of BM in the right tibia was established and then confirmed by ultrasound images as previously described[6]. BALB/c mice (female, aged 6-8 weeks, 20-25 g) were anesthetized by

intraperitoneal injection of 60 µl pentobarbital sodium (w/v at 2.5%). Then, a 29 gauge insulin syringe was drilled into the medullary cavity of the tibia from the tibial plateau, and 1×10^5 4T1 cells in 20 µl PBS were implanted into the medullary cavity of the right tibia using another 29 gauge insulin syringe.

Daily ultrasound images of the legs were acquired on a Siemens S3000 US scanner (Siemens, Mountain View, CA) from the 3rd day postmodeling. The following features observed in the US images confirmed that the mouse model of BM was established successfully: 1) the tibial cortex was discontinuous or rough, 2) the maximum diameter of the model leg increased >1.0 mm compared with the control leg, and 3) the distance between the tibial tuberosity and the skin above increased > 0.2 mm compared with that in the control.
BM-bearing mice (as determined by ultrasound) were used for imaging and therapeutic experiments.

6.2 Bone-Targeting Ability of ZZF-8 NPs *in vivo*

To evaluate the efficiency of the bone-targeting ability of ZZF-8 nanocarrier systems, Cy5.5 (Ex=675 nm, Em=694 nm) was loaded into ZZF-8 NPs (Cy5.5@ZZF-8) and 150 µl of a 1 mg/ml Cy5.5@ZZF-8 NPs solution was injected intravenously via the tail vein to observe the distribution of the NPs *in vivo*. The following three groups of mice were evaluated by fluorescence imaging: 1) normal mice with Cy5.5@ZIF-8, 2) BM-bearing mice with Cy5.5@ZIF-8 and 3) BM-bearing mice with Cy5.5@ZZF-8. An *in vivo* imaging system (IVIS, Perkin Elmer) with 675 nm excitation was used to image the mice at different time points (6, 10, 16, 24 and 48 h) to identify the time point at which the accumulation efficiency of the NPs at the tumor site was highest. All mice were sacrificed at the time point with the highest accumulation of NPs. Afterward, the legs were removed for imaging, including the muscles. The kidney, lung, spleen, heart and liver were also harvested and imaged. The region of irradiation (ROI) was analyzed by IVIS Spectrum imaging software.

6.3 *In Vivo* Anticancer Efficacy Assessment

BM-bearing mice were randomly allocated into 6 groups (n=4): 1) ICG/Cyt c@ZZF-8 + laser, 2) ICG@ZZF-8 + laser, 3) ICG/Cyt c@ZZF-8 without laser, 4) ICG/Cyt c@ZIF-8 + laser, 5) solution of Cyt c + laser and 6) PBS without laser. A 150 µl aliquot of saline or NP solution was intravenously injected into the mice (equivalent ICG concentration of 132 µg/ml, NP concentration of 2 mg/ml, Cyt c concentration of 92 µg/ml) on day 0 and day 3. 16 hours after injection, the BM sites were exposed a 780 nm laser (0.5 W/cm^2, 1 min on, 1 min off and then 1 min on, total 3 min) or remained unexposed in the control groups. The circumference of the proximal tibia of each mouse was recorded by an electronic caliper every day during treatment. The number of days each mouse survived was recorded. Additionally, the important organs (heart, liver, spleen and kidney) and the legs removed from the proximal femur were fixed in 4% paraformaldehyde after the mice died. The legs were imaged with microcomputed tomography (micro-CT, Viva CT-80). Bone volume (BV), trabecular number (Tb. N), bone surface/bone volume ratio (BS/BV), and percent bone volume (bone volume/tissue volume) were all analyzed by SkyScan CT analysis software (SCANCO Medical AG, Zurich, Switzerland), with the region of interest set to 50 slides below the growth plate to evaluate the extent of bone destruction.[7] Afterward, the major organs and legs were sectioned for staining with hematoxylin and eosin (H&E) and histologically analyzed using a microscope.

TRAP assays were also performed on the leg tissue sections to observe osteoclasts in the lesions.

To verify the biosafety of ICG/Cyt c@ZZF-8, 150 μl of ICG/Cyt c@ZZF-8 NP solution (1 mg/ml) was injected into mice via the tail vein on days 0 and 3. Another group of mice was injected with PBS as a control. Then, we collected blood samples from the submandibular on day 7 for blood chemistry tests and routine blood analyses.

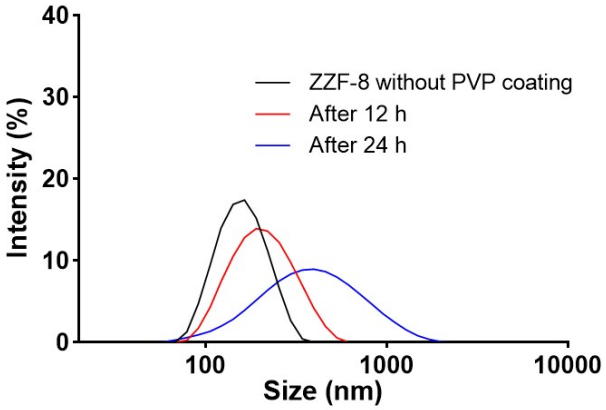

Figure S1. Size distribution results of ZZF-8 NPs without PVP coating measured by DLS, and re-test after let it stand for 12 and 24 h.

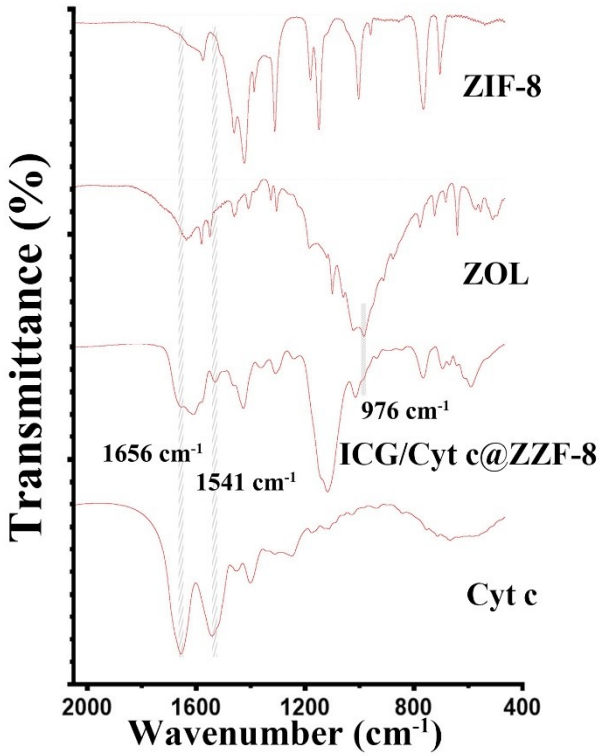

Figure S2. The FT-IR spectra detection of the ZIF-8 NPs, ZOL, ICG/Cyt c@ZZF-8 NPs and Cyt c.

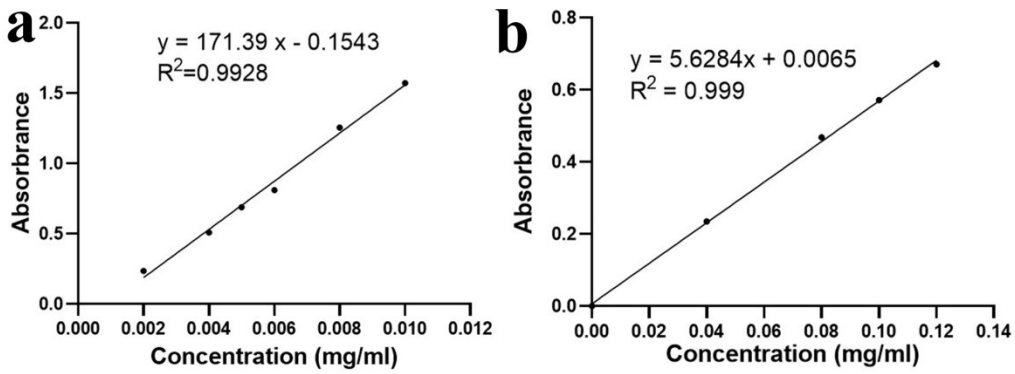

Figure S3. (a) Standard linear calibration curves of ICG (absorption at 780 nm). (b) Standard linear calibration curves of ABTS with different concentrations of Cyt c (absorption at 417 nm).

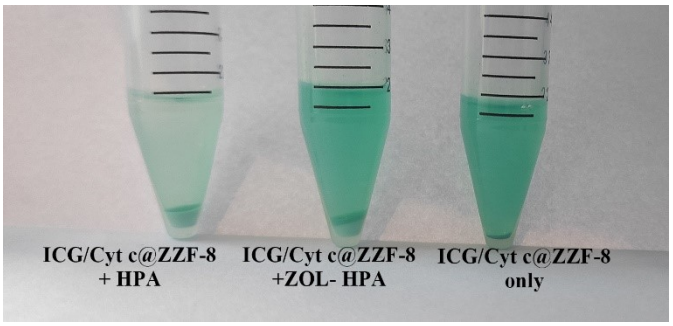

Figure S4. Photograph of 3 groups after centrifugation in HPA-binding assays.

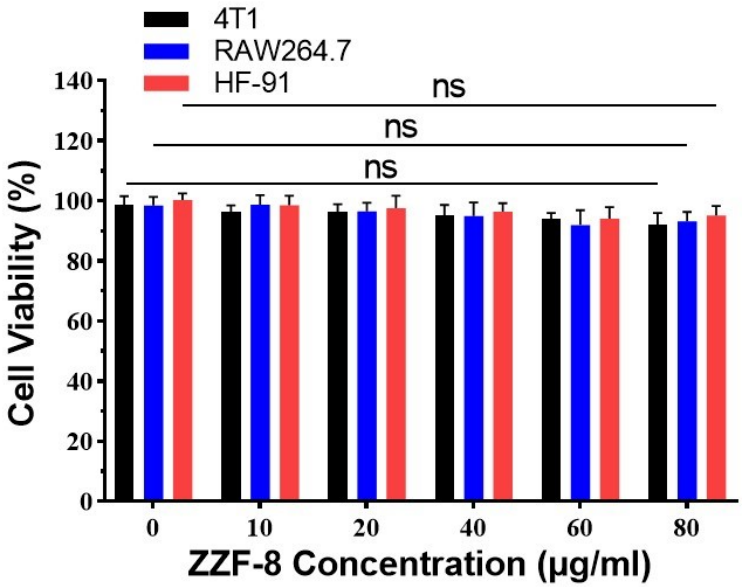

Figure S5. Relative cell viability of 4T1, RAW264.7 cells of mice and HF-91 cells of human incubated with ZZF-8 NPs in various concentrations.

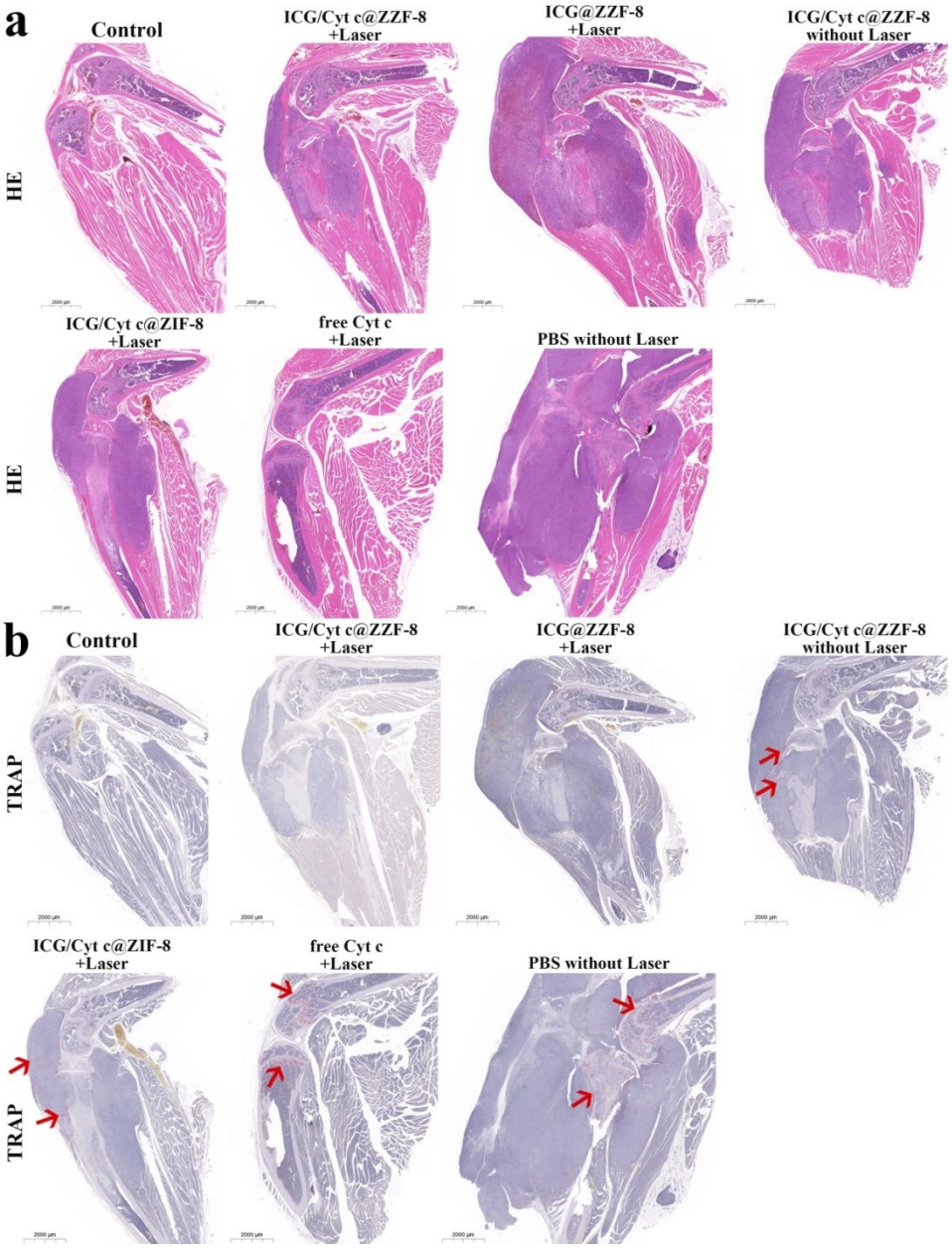

Figure S6. (a) H&E staining of leg tissue slices in experimental and control groups (scale bar, 2000 μm), (b) TRAP assays of tumor tissue slices after different treatments in experimental and control groups (scale bar, 2000 μm).

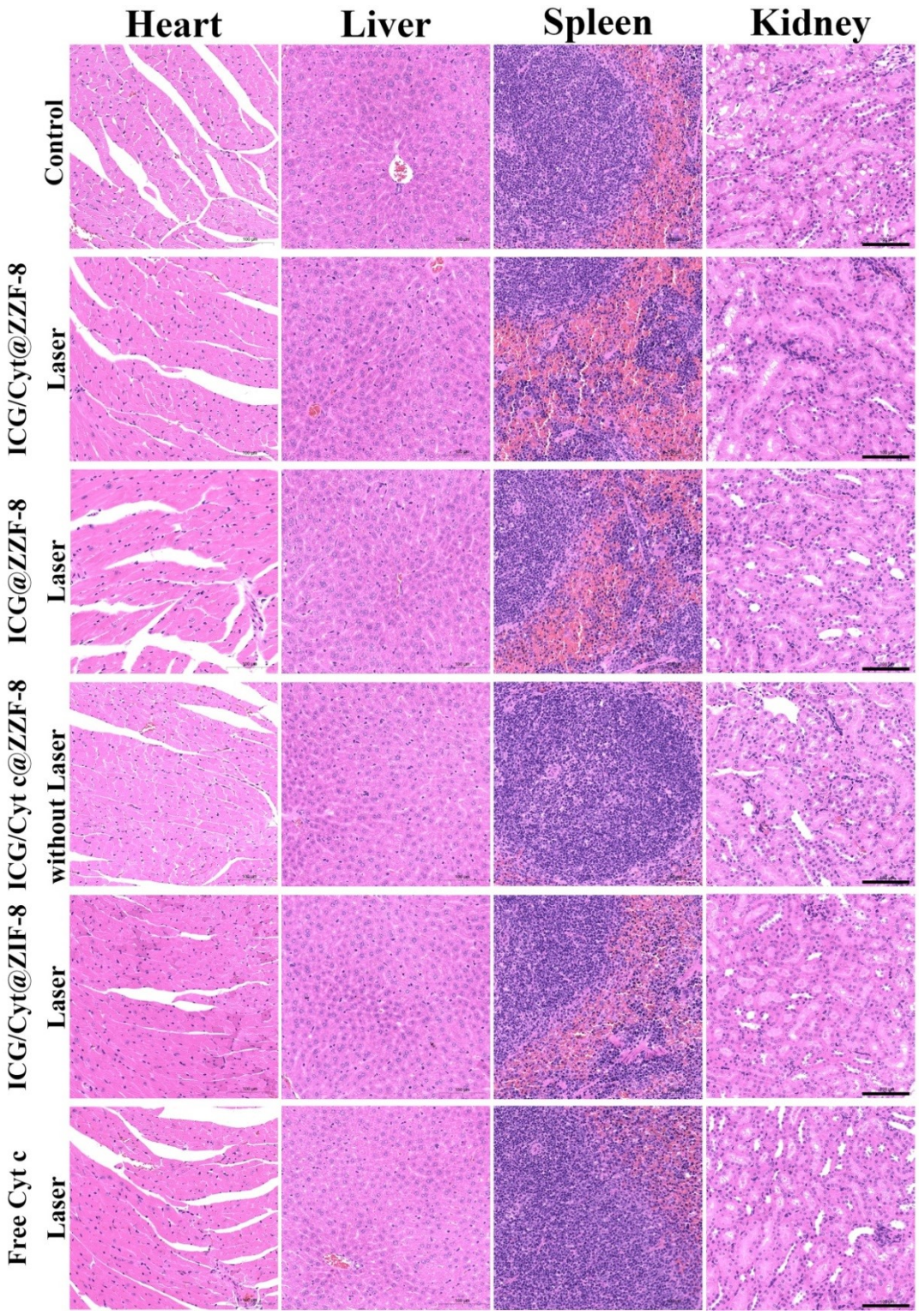

Figure S7. H&E staining of major organs (heart, liver, spleen and kidney) dissected from mice after all experimental operations, include control group and different treatment groups (scale bar, 100 μm).

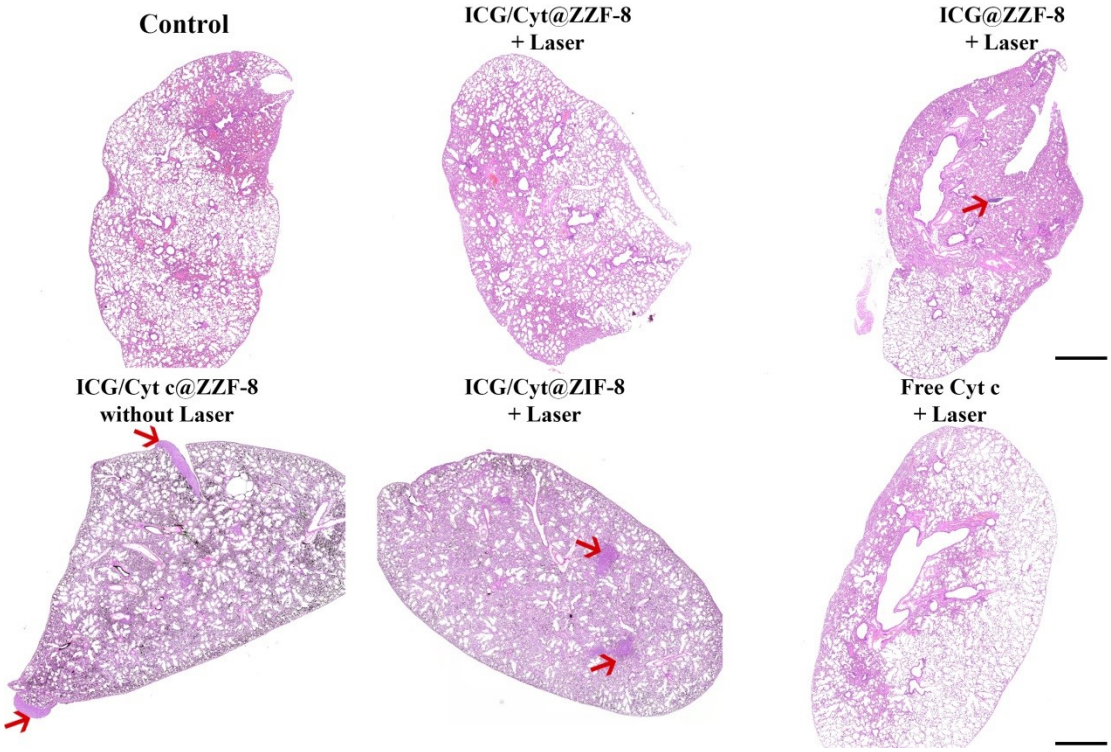

Figure S8. H&E staining of lung dissected from mice after experimental operations (scale bar, 1000 μm).

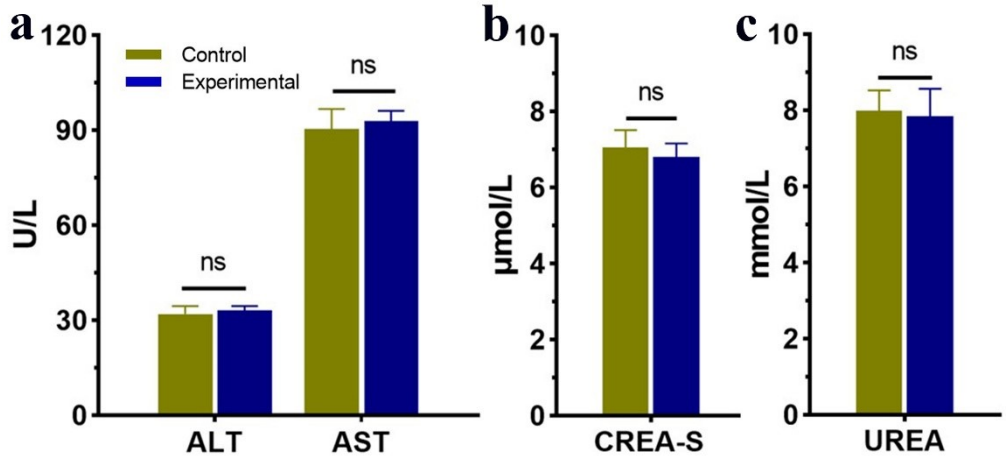

Figure S9. The blood biochemical analysis of health mice intravenously injected with ICG/Cyt c@ZZF-8 NPs (measured at day 7, marked as experimental) and PBS (measured at day 7, marked as control), liver function: alanine transaminase (ALT), aspartate aminotransferase (AST), kidney function: Urea (UREA), serum creatinine (CREA).

References

[1] X. Wang, D. Miao, X. Liang, J. Liang, C. Zhang, J. Yang, D. Kong, C. Wang, H. Sun, Nanocapsules engineered from polyhedral ZIF-8 templates for bone-targeted hydrophobic drug delivery, Biomater Sci 5(4) (2017) 658-662.

[2] B. Huang, S. Chen, W. Pei, Y. Xu, Z. Jiang, C. Niu, L. Wang, Oxygen-Sufficient Nanoplatform for

Chemo-Sonodynamic Therapy of Hypoxic Tumors, Front Chem 8 (2020) 358.
[3] S. Chen, B. Huang, W. Pei, L. Wang, Y. Xu, C. Niu, Mitochondria-Targeting Oxygen-Sufficient Perfluorocarbon Nanoparticles for Imaging-Guided Tumor Phototherapy, Int J Nanomedicine 15 (2020) 8641-8658.
[4] L. Ding, X. Lin, Z. Lin, Y. Wu, X. Liu, J. Liu, M. Wu, X. Zhang, Y. Zeng, Cancer Cell-Targeted Photosensitizer and Therapeutic Protein Co-Delivery Nanoplatform Based on a Metal-Organic Framework for Enhanced Synergistic Photodynamic and Protein Therapy, ACS Appl Mater Interfaces 12(33) (2020) 36906-36916.
[5] M. Ye, Y. Han, J. Tang, Y. Piao, X. Liu, Z. Zhou, J. Gao, J. Rao, Y. Shen, A Tumor-Specific Cascade Amplification Drug Release Nanoparticle for Overcoming Multidrug Resistance in Cancers, Adv Mater 29(38) (2017).
[6] Z. Jiang, J. Li, S. Chen, Q. Guo, Z. Jing, B. Huang, Y. Pan, L. Wang, Y. Hu, Zoledronate and SPIO dual-targeting nanoparticles loaded with ICG for photothermal therapy of breast cancer tibial metastasis, Sci Rep 10(1) (2020) 13675.
[7] H. Qiao, Z. Cui, S. Yang, D. Ji, Y. Wang, Y. Yang, X. Han, Q. Fan, A. Qin, T. Wang, X.-P. He, W. Bu, T. Tang, Targeting Osteocytes to Attenuate Early Breast Cancer Bone Metastasis by Theranostic Upconversion Nanoparticles with Responsive Plumbagin Release, Acs Nano 11(7) (2017) 7259-7273.